Ferromagnetism and structural transformations caused by Cr intercalation into $TiTe_2$

2009 J. Phys.: Condens. Matter 21 506002

(http://iopscience.iop.org/0953-8984/21/50/506002)

J. Phys.: Condens. Matter **21** (2009) 506002 (8pp) doi:10.1088/0953-8984/21/50/506002

Ferromagnetism and structural transformations caused by Cr intercalation into $TiTe_2$

N V Baranov[1,2], V G Pleshchev[2], N V Selezneva[2], E M Sherokalova[2], A V Korolev[1], V A Kazantsev[1] and A V Proshkin[1,2]

[1] Institute of Metal Physics, Russian Academy of Science, 620041 Ekaterinburg, Russia
[2] Institute of Physics and Applied Mathematics, Ural State University, 620083 Ekaterinburg, Russia

E-mail: nikolai.baranov@usu.ru

Received 21 September 2009, in final form 22 October 2009
Published 23 November 2009
Online at stacks.iop.org/JPhysCM/21/506002

Abstract

Crystal structure investigations, electrical resistivity, and magnetic measurements have been performed for polycrystalline samples of intercalated compounds Cr_xTiTe_2 with a Cr concentration up to $x = 0.65$. According to the room-temperature x-ray diffraction study of Cr_xTiTe_2, the initial hexagonal crystal structure transforms to a monoclinic one with increasing Cr content up to $x \geqslant 0.5$ due to the ordering of Cr ions. The intercalation results in the change of the resistivity behavior in Cr_xTiTe_2 from metal-like at $x = 0$ to insulator-like above $x = 0.33$ and leads to ferromagnetic ordering of Cr magnetic moments at $x \geqslant 0.5$. For the compound $Cr_{0.25}TiTe_2$, structural transformations and anomalous resistivity behavior are observed around 230 K, which cannot be explained only by the order–disorder transition within the subsystem of intercalated Cr ions. Structural changes within Te–Ti–Te sandwiches associated with charge density wave instability are suggested to be involved in this phase transition as well.

(Some figures in this article are in colour only in the electronic version)

1. Introduction

Layered compounds based on transition metal (T) dichalcogenides have been a subject of particular interest for investigations in the field of the physics and chemistry of two-dimensional states. The TX_2 (X = S, Se, Te) compounds have highly anisotropic physical properties and reveal unique electronic properties such as a variety of charge density wave (CDW) and superconducting transitions [1, 2]. Among the TX_2 compounds, great attention has been paid to the study of titanium dichalcogenides. The TiX_2 (X = S, Se, Te) compounds consist of a hexagonal layer of Ti atoms arranged between two similar layers of chalcogen atoms, forming the basic X–Ti–X tri-layer. The X–Ti–X sandwiches are coupled by relatively weak van der Waals (vdW) forces while the atoms within the sandwiches are coupled by strong covalent bonds [1, 2]. Within the family of titanium dichalcogenides, the most attention was paid to the study of the crystal structure and physical properties of the $TiSe_2$ compounds because of the existence of a structural phase transition induced by a charge density wave (CDW) below the critical temperature $T_t \approx 200$ K [3].

Unlike $TiSe_2$, some inconsistency exists in the literature in respect to the presence of the CDW state in $TiTe_2$. The indications on the presence of a first-order phase transition of the CDW type in $TiTe_2$ were found by de Boer *et al* [4]. An abrupt change of the magnetic susceptibility with a remarkable hysteresis was observed around 150 K on a single crystal of $TiTe_2$ in [4]. However, this observation was not reproduced in other studies [5, 6] probably because of the difference in preparation methods and in the stoichiometry of crystals. Above 5 K, the temperature dependences of the electrical resistivity for $TiTe_2$ are found to be typical for semimetals [4–6], which is consistent with band structure calculations and photoemission experiments [6, 7]. The electronic structure of $TiTe_2$ is formed by partial overlap

of the Te 5p derived valence states with the Ti 3d derived conduction states [6, 7]. Within the TiX_2 family, the lattice parameter c increases from 5.699 Å for TiS_2 up to 6.491 Å for $TiTe_2$ [8, 9] with increasing atomic number of chalcogen. The estimation of the minimal distance d_{X-X} between positions of chalcogen atoms belonging to adjacent X-layers shows that the van der Waals gap width increases by about 12% when going from TiS_2 to $TiTe_2$. However, despite the larger 'geometrical' width d_{X-X}, the 'physical' width of the vdW gap in $TiTe_2$ is lower than in TiS_2 because of a larger spatial extension of Te^{2-} 5p-orbitals and higher ionic radius (by about 20% in comparison with S^{2-} [10]). This implies the strengthening of the interaction between X–Ti–X sandwiches with increasing atomic number of chalcogen, which may affect the properties of intercalated compounds based on TiX_2 matrixes. It is well known that the intercalation of foreign atoms or molecules into the layered crystal lattices is an effective tool for substantial modification of their physical properties. In particular, the recent studies of Cu_xTiSe_2 compounds have shown that the insertion of Cu atoms between Se–Ti–Se tri-layers suppresses the CDW state and leads to the appearance of the superconductivity [11]. The intercalation of transition metal (M) atoms with non-full 3d electron shells results in the presence of different magnetic states in M_xTiX_2 at low temperatures starting from spin-glass and cluster-glass at low intercalant concentrations ($x < 0.33$) up to ferromagnetic or antiferromagnetic arrangements of magnetic moments at $x > 0.33$ [12–15].

The aim of the present paper is to study the influence of the Cr intercalation on the crystal structure, magnetic, and other physical properties of titanium ditelluride. The polycrystalline Cr_xTiTe_2 samples are synthesized with various intercalant concentrations up to $x = 0.65$. Detailed x-ray diffraction measurements, as well as the measurements of different properties including magnetic susceptibility, magnetization, electrical resistivity, specific heat, and thermal expansion have been performed in order to clarify the different mechanisms which are responsible for the crystal structure modifications and substantial changes in the behavior of physical properties.

2. Experimental details

The Cr_xTiTe_2 compounds with $x = 0$, 0.1, 0.25, 0.33, 0.5, and 0.65 were prepared by chemical reaction inside a sealed quartz tube in two stages. At first, the parent compounds $TiTe_2$ was synthesized by heat treatment of a mixture of starting materials at 800 °C for one week. At the second stage the mixtures of Cr and $TiTe_2$ powders were pressed into cylindrical pellets and annealed at the same conditions followed by cooling down through removal of the tube from the oven into air. The intercalated Cr_xTiTe_2 compounds with Cr concentrations up to $x = 0.65$ are found to be single phase. The quality of all samples was checked by powder x-ray diffraction analysis by using a Bruker D8 Advance diffractometer with Cu Kα radiation. For Rietveld refinements of the crystal structure, the FULLPROF program was used [16]. The electrical resistivity of the polycrystalline samples of Cr_xTiTe_2 was measured from 4.2 to 300 K by a conventional four-contact dc method. The ac and dc magnetic susceptibility as well as the magnetization were measured by means of a Quantum Design superconducting quantum interference device (SQUID) magnetometer in the temperature interval from 2 up to 300 K. The specific heat measurements were performed using an adiabatic calorimeter. The temperature dependence of the linear coefficient of thermal expansion was measured on polycrystalline samples using the dilatometer DL-1500 RHP/DL-1500-H (UCVAC/SINKU).

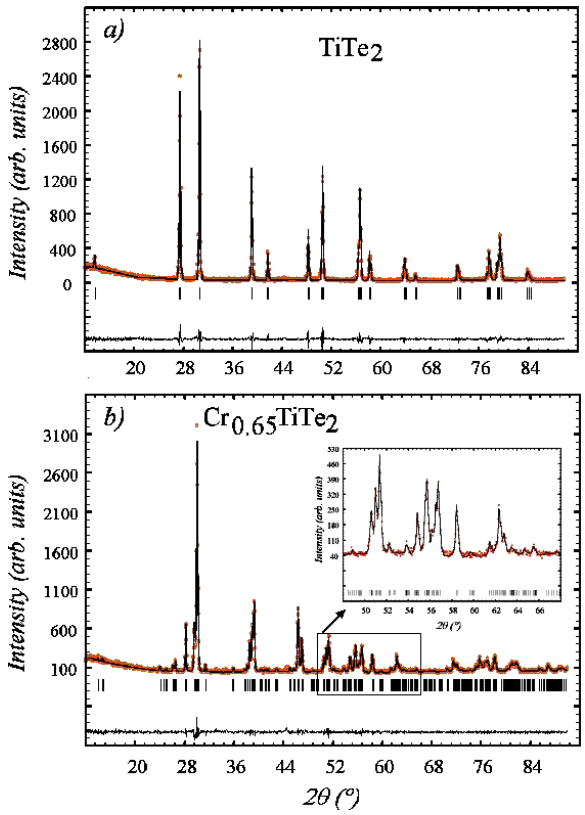

Figure 1. Observed (symbols) and calculated (line) x-ray diffraction patterns for $TiTe_2$ (*a*) and $Cr_{0.65}TiTe_2$ (*b*) at room temperature. The difference between calculated and observed intensities is shown in the bottom of the figure. Vertical bars indicate the calculated Bragg peaks positions.

3. Results and discussion

3.1. The room-temperature crystal structure

Figure 1(a) shows the x-ray powder diffraction pattern obtained at room temperature for the parent $TiTe_2$. Analogous patterns without visible changes were obtained for all Cr_xTiTe_2 compounds with intercalant concentrations $x < 0.5$. These patterns correspond to the single-phase GdI_2 type crystal structure ($P\bar{3}m1$ space group) as for the parent $TiTe_2$ compound. The lattice parameters obtained for our $TiTe_2$ sample ($a = 3.770$ Å, $c = 6.490$ Å) are in a good agreement with previous data [8, 9]. At $x \geqslant 0.5$, the ordering of Cr ions in vdW gaps leads to the appearance of a superlattice $\sqrt{3}a_0 \times a_0 \times 2c_0$ (a_0 and c_0 are the hexagonal cell parameters) which can be clearly seen from figure 1(b), which displays the x-ray diffraction pattern for $Cr_{0.65}TiTe_2$. According to our refinement ($wRp = 2.36\%$) this compound exhibits a monoclinic type

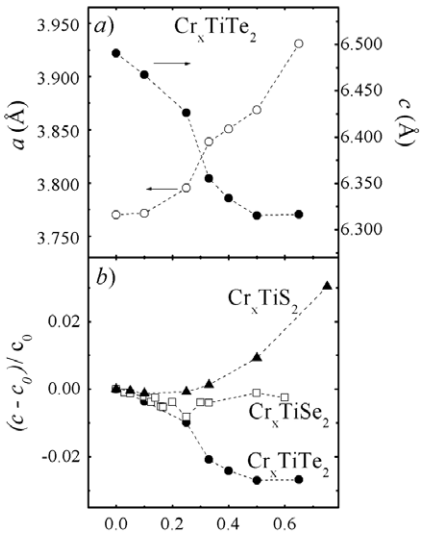

Figure 2. Lattice parameters a (open circles) and c (full circles) of Cr_xTiTe_2 compounds (a) and the $(c - c_0)/c_0$ value for Cr_xTiX_2 families (X = S, Se, Te) (b) as a function of the Cr concentration. The data for Cr_xTiS_2 and Cr_xTiSe_2 are taken from [20, 14], respectively.

crystal structure (space group $I12/m1$) with lattice parameters $a = 6.806$ Å, $b = 3.8657$ Å, $c = 12.629$ Å, $\beta = 89.12°$. Such a superstructure caused by ordering of M atoms was also observed in some M_xTiS_2 [17] and M_xTiSe_2 [18, 19] compounds.

As follows from figure 2, which displays the calculated lattice parameters, the insertion of Cr atoms into the $TiTe_2$ matrix leads to the contraction of the crystal lattice perpendicular to layers and to the growth of the interatomic distance within layers. Such lattice deformations were also observed in M_xTiSe_2 compounds intercalated with 3d metal atoms except Mn at the intercalant concentrations $x < 0.33$ (see [21] and references therein). The reduction of the average interlayer distance in M_xTiX_2 was attributed to the formation of covalent-like bonds between Se–Ti–Se sandwiches through inserted M ions. As it turned out, the influence of the Cr intercalation on the crystal lattice deformation depends on the type of chalcogen ion in TiX_2. Figure 2(b) shows the relative changes of the lattice parameter c for Cr_xTiTe_2, Cr_xTiSe_2 and Cr_xTS_2 families. As is seen, unlike the TiS_2 compound, the intercalation of which expands the lattice in the c direction, the insertion of Cr ions into $TiTe_2$ shows the opposite influence. An intermediate case is observed for Cr_xTiSe_2: the c parameter decreases with increasing Cr content up to $x = 0.25$, while further Cr intercalation into $TiSe_2$ is accompanied by the growth of the average interlayer distance. The different influence of the Cr intercalation on the TiX_2 lattices may originate in the difference of the ionicity/covalency ratio of Cr bonds in TiX_2 matrixes. One can suggest that the degree of the covalency of these bonds increases when going from Cr_xTiS_2 to Cr_xTiTe_2. This is consistent with the evolution of chemical bonding within X–Ti–X sandwiches. As was shown in [9], the covalency of chemical bonding increases, while the ionicity decreases in the series of TiS_2–$TiSe_2$–$TiTe_2$.

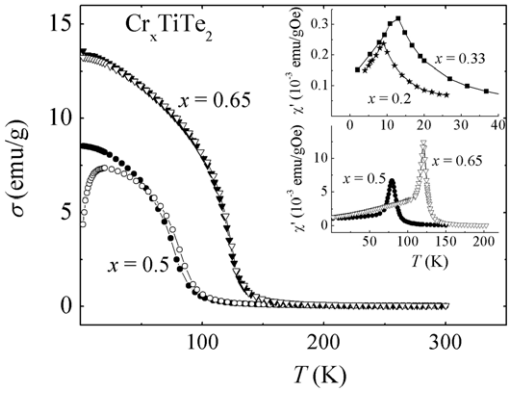

Figure 3. Temperature dependences of the magnetization for highly intercalated Cr_xTiTe_2 compounds ($x = 0.5$; 0.65) at $H = 1$ kOe. Full and open symbols correspond to the FC and ZFC regimes, respectively. Insets show the real part of the ac susceptibility for Cr_xTiTe_2 at various Cr concentrations.

3.2. Magnetic properties

The intercalation of Cr atoms exhibiting an open 3d electron shell modifies substantially the magnetic properties of $TiTe_2$. The measurements of the temperature dependence magnetization at $H = 1$ kOe have revealed a ferromagnetic behavior for Cr_xTiTe_2 compounds with Cr concentrations $x = 0.5$ and 0.65 (see figure 3). The Curie temperatures for these compounds were determined to be about 78 K and 120 K respectively from the ac susceptibility data which are displayed in the inset in figure 3. As for the Cr_xTiTe_2 compounds with lower Cr concentrations, their magnetic states can be characterized as spin-glass or cluster-glass states [22]. According to [22], the magnetic susceptibility for the compounds with $x < 0.33$ exhibits an essential hysteresis when the measurements were made on a sample cooled in zero magnetic field (ZFC) or on a sample cooled in an applied field (FC). Moreover, the ac susceptibility of Cr_xTiTe_2 with $x = 0.2$ and 0.25 is found to be frequency dependent around the freezing temperatures T_f [22]. The presence of a ferromagnetic order in Cr_xTiTe_2 at $x \geqslant 0.5$ is confirmed by the magnetization measurements at low temperatures. As can be seen from figure 4, the field dependences of the magnetization measured at 2 K for $Cr_{0.5}TiTe_2$ and $Cr_{0.65}TiTe_2$ show a clear saturation above 20 kOe. From magnetization data, the value of the average magnetic moment of Cr ions in the magnetically ordered state (μ_{Cr}) is estimated to be about 2.2 μ_B and 2.4 μ_B at $x = 0.5$ and $x = 0.65$, respectively. These values are close to that observed for the antiferromagnetic compound $Cr_{0.5}TiSe_2$ in the field-induced ferromagnetic state (~2.3 μ_B [14]). In both compounds, this magnetic moment is lower than the expected value $\mu_{Sat} = 3\ \mu_B$ in the fully saturated state for Cr^{3+} at low temperatures. There are several origins which may lead to the reduced μ_{Cr} values observed on a polycrystalline sample: (i) the presence of substantial magnetocrystalline anisotropy; (ii) the non-collinearity of the magnetic structure; and (iii) the partial delocalization of Cr 3d electrons and hybridization effects. Magnetization measurements on single crystalline samples and

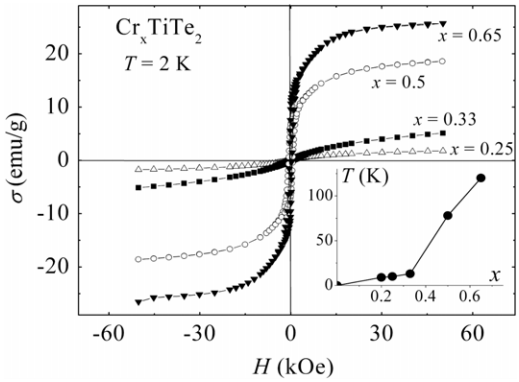

Figure 4. Field dependences of the magnetization at $T = 2$ K for Cr_xTiTe_2 with different intercalant concentrations. The inset shows the concentration dependence of the magnetic critical temperature.

Table 1. The effective magnetic moment μ_{eff}, paramagnetic Curie temperature Θ_p, and critical magnetic temperatures (T_f, T_C) obtained from paramagnetic susceptibility data for Cr_xTiTe_2 compounds.

x	0.1	0.2	0.25	0.33	0.5	0.65
μ_{eff} /Cr (μ_B)	4.1	3.9	4.1	3.8	4.1	4.1
Θ (K)	~0	6	8	15	115	160
T_f, T_C (K)	3	9	10	12	78	120

the detailed neutron diffraction studies are needed in order to reveal the main reasons.

For all Cr_xTiTe_2 compounds, the temperature dependences of the magnetic susceptibility $\chi(T)$ in the paramagnetic state are observed to obey the expression $\chi = \chi_0 + C/(T - \Theta_p)$. The temperature independent term χ_0 includes the diamagnetic contribution and paramagnetic contribution from delocalized electrons. The values of the effective magnetic moment μ_{eff} and paramagnetic Curie temperature Θ_p obtained by fitting as well as the critical temperatures T_f and T_C are listed in table 1. The μ_{eff} values for Cr ions intercalated into $TiTe_2$ are found to lie between 3.8 and 4.1 μ_B, i.e. close to the expected $\mu_{\text{eff}} = g\mu_B[S(S+1)]^{1/2} = 3.87\ \mu_B$ calculated at $g = 2$ for Cr^{3+}. These data show that 3d electrons of Cr ions intercalated into the $TiTe_2$ matrix remain quite well localized, which is consistent with band structure calculations and angle-resolved photoemission spectroscopy measurements performed for the $Cr_{0.33}TiTe_2$ compound [23]. According to [23] the Cr intercalation results in the formation of a narrow almost non-dispersion band of hybridized Cr 3d–Ti 3d states. This band is observed to lie at about 1 eV below the Fermi level.

As follows from table 1, the Θ_p values are positive for all compounds at $x > 0.1$, which is indicative of the dominating ferromagnetic exchange. Both the Θ_p value and the Curie temperature T_C starts to grow substantially with increasing Cr concentration above $x = 0.33$; this is clearly seen from the inset in figure 4. The positive Θ_p values were also observed in Cr_xTiSe_2 compounds at a Cr content above $x = 0.33$, while these compounds exhibit an antiferromagnetic order which can be destroyed by application of a relatively small magnetic field (10–20 kOe) [14]. The latter was

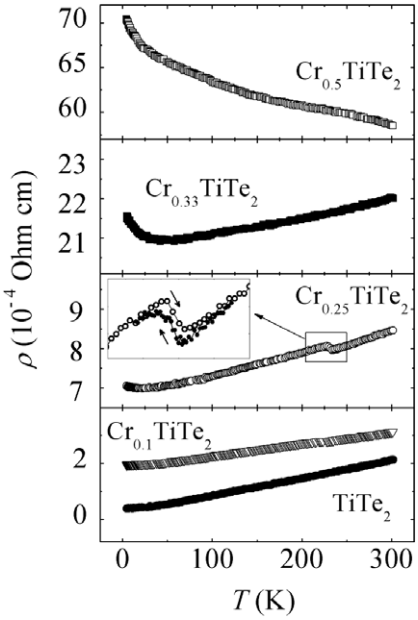

Figure 5. Temperature dependences of the electrical resistivity of Cr_xTiTe_2 compounds at various Cr concentrations. The inset shows a part of the $\rho(T)$ dependence for $x = 0.25$ in detail.

attributed to a weak antiferromagnetic exchange interaction between ferromagnetically ordered neighbor Cr layers. Unlike Cr_xTiSe_2, in highly intercalated Cr_xTiTe_2 compounds, the ferromagnetic exchange dominates between and within Cr layers.

3.3. Electrical resistivity

Figure 5 shows the evolution of the electrical resistivity of $TiTe_2$ with Cr intercalation. As can be seen, the increase of the Cr concentration leads to the growth of the resistivity values while the metallic character of $\rho(T)$ dependences persists in Cr_xTiTe_2 up to $x = 0.33$. This is despite the growth of the electron concentration since the guest Cr atoms donate electrons to the host material, becoming trivalent ions. According to [4] the electrical resistivity of the parent compound $TiTe_2$ can be described as the sum of the residual resistivity, electron–electron, electron–phonon, and impurity scattering contributions. The electron–electron and electron–phonon contributions are suggested to be responsible for the monotonous growth of the resistivity with increasing temperature in this case as in other metallic systems [4]. The metallic resistivity behavior observed for the intercalated Cr_xTiTe_2 compounds with $x < 0.33$ at temperatures above 50 K is associated apparently with the same contributions. The appearance of a minimum in the $\rho(T)$ dependences in these compounds in the low-temperature region may be attributed to the presence of an additional contribution which increases with lowering temperature. In our opinion, this extra contribution to the total resistivity has a magnetic origin at $x < 0.33$ and results from the scattering of conduction electrons on magnetic moments of clusters, bearing in mind that the magnetic state of these compounds is of a cluster-glass type (see above). This contribution increases with lowering temperature owing to the

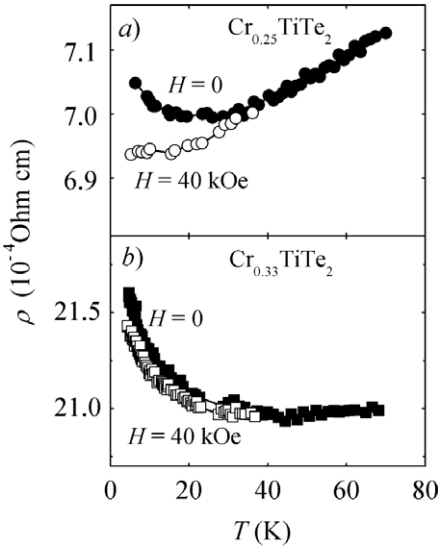

Figure 6. ρ versus T dependences for $Cr_{0.25}TiTe_2$ (*a*) and $Cr_{0.33}TiTe_2$ (*b*) measured without magnetic field (full symbols) and at $H = 40$ kOe (open symbols).

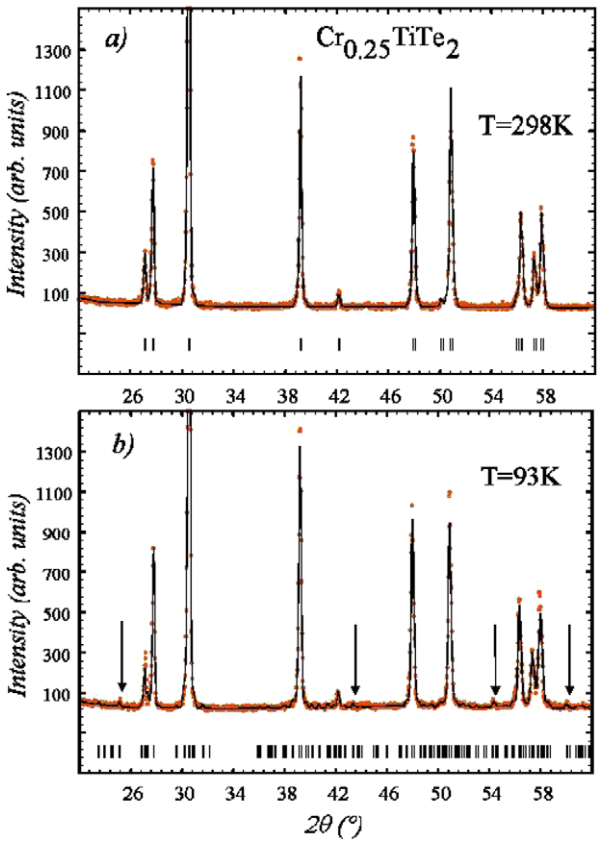

Figure 7. Observed (symbols) and calculated (line) x-ray diffraction patterns for $Cr_{0.25}TiTe_2$ at temperatures 298 K (*a*) and 93 K (*b*). Vertical bars indicate the calculated Bragg peak positions for the CdI_2 type (*a*) and monoclinic (*b*) structures.

growth of the number and volume of magnetic clusters formed by intercalated Cr ions as in diluted alloys with magnetic clustering [24]. The application of the magnetic field 40 kOe leads to the disappearance of the resistivity minimum because of the suppression of this extra contribution (shown in figure 6). As follows from figure 5, the low-temperature upturn of the resistivity becomes more pronounced with the growth of the Cr concentration up to $x = 0.33$. Further intercalation leads to insulator-like behavior which is observed for $Cr_{0.5}TiTe_2$.

Such changes in the resistivity behavior in Cr_xTiTe_2 with increasing intercalant concentration above $x = 0.33$ may be attributed to an increase in the degree of the conduction electron localization. The magnetic scattering has apparently a lesser influence at $x \geqslant 0.33$, as can be seen from figure 6(b), which displays a low-temperature part of the $\rho(T)$ dependence for $Cr_{0.33}TiTe_2$. For this compound, the resistivity starts to grow with cooling at much higher temperature (∼50 K) than the freezing temperature ($T_f \sim 12$ K). The magnetic field 40 kOe does not suppress the upturn of the resistivity in $Cr_{0.33}TiTe_2$, the resistivity minimum remains quite well pronounced after application of a magnetic field. Above 40 K, the application of a magnetic field up to 40 kOe does not change noticeably the resistivity of Cr_xTiTe_2 samples, therefore these data were not recorded. It should be noted that the change from metal-like to insulator-like resistivity behavior was also observed in some other transition metal dichalcogenides M_xTX_2 at the intercalation of 3d metal atoms into vdW gaps [25] or at the substitution $M_yT_{1-y}X_2$ (T = Ta, V; M = Fe) [26, 27]. Such a behavior of the resistivity in these compounds was attributed to the Anderson-type localization by the random potential of M atoms.

Another feature of the electrical resistivity should be mentioned. There is a small step on the $\rho(T)$ curve for $Cr_{0.25}TiTe_2$ at temperatures about 230 K (see figure 5). The sharp growth of ρ by about 2% with decreasing temperature observed for $Cr_{0.25}TiTe_2$ between 230 and 225 K may be indicative of the change in the electronic structure of this compound. Below and above this temperature interval, the resistivity shows a conventional metal-type near-linear temperature dependence with the same slope. It seems that such an anomaly should be more pronounced on the $\rho(T)$ dependence for a single crystalline sample. In order to check this observation we have synthesized several polycrystalline samples with the given composition. In all the samples, such an anomalous behavior of the resistivity was observed in the region ∼225–240 K. The presence of the thermal hysteresis about 3 K on $\rho(T)$ dependences (shown in the inset in figure 5) is indicative of the first-order type of such a metal–metal transition.

3.4. Structural phase transition in $Cr_{0.25}TiTe_2$

In order to reveal the origins of the anomalous change of the resistivity observed for $Cr_{0.25}TiTe_2$ around 230 K we have performed detailed x-ray diffraction measurements on a powder sample in a wide temperature interval. Figure 7 shows the x-ray patterns taken at room temperature and at $T = 93$ K, i.e. far below the transition temperature. The decrease of the temperature below 240 K is observed to be accompanied by the appearance of additional superstructure reflections on the diffraction pattern (shown by arrows). The temperature evolution of some extra reflections is shown in

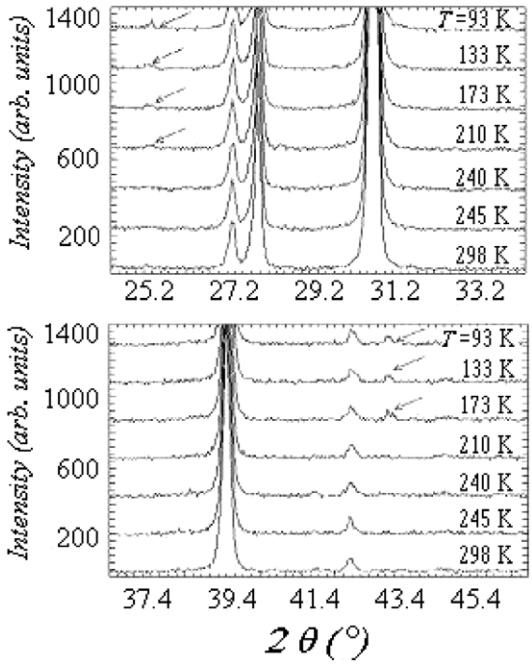

Figure 8. X-ray diffraction patterns in the vicinity of some reflections at various temperatures. The additional reflections are indicated by arrows.

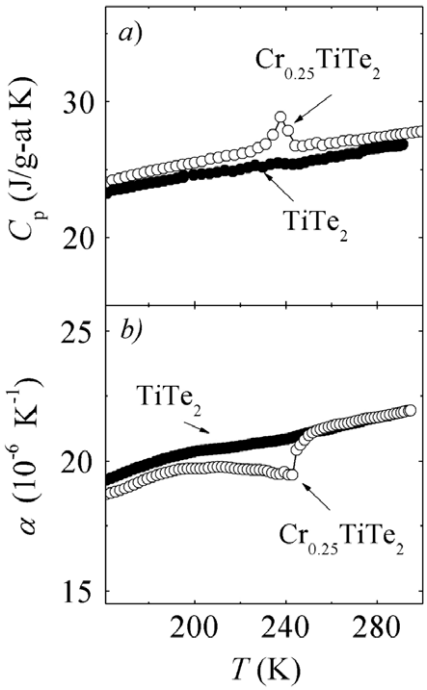

Figure 10. Temperature dependences of the specific heat (*a*) and linear thermal expansion coefficient (*b*) for $TiTe_2$ and $Cr_{0.25}TiTe_2$.

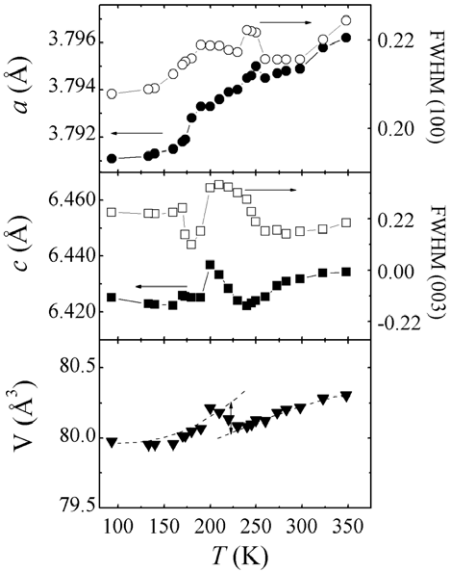

Figure 9. Temperature variation of the FWHM for (100) and (003) reflections, the lattice parameters *a* and *c* and the volume calculated for a hexagonal unit cell of $Cr_{0.25}TiTe_2$.

figure 8. Together with the appearance of new additional reflections, the anomalous changes of the full width at half maximum (FWHM) was revealed for some Bragg reflections with lowering temperature. The temperature dependences of the FWHM for (100) and (003) reflections, the lattice parameters *a* and *c* as well as the volume of a hexagonal unit cell are displayed in figure 9. The values of FWHM start to grow with decreasing temperature below ∼260 K, i.e. well above the critical temperature.

The anomalous behavior of FWHM is more pronounced for reflections of (00*l*) type and extends for a wide temperature interval (from 260 K down to ∼160 K). As shown in figure 9, the unit cell volume decreases with lowering temperature from 298 K down to 240 K. However, on further cooling, the lattice expands by about 0.24% and then the volume shows a downward tendency below 200 K. These data clear indicate that the above-mentioned resistivity anomaly in $Cr_{0.25}TiTe_2$ is accompanied by structural changes. The x-ray diffraction pattern measured at $T = 93$ K can be described according to the monoclinic cell ($F12/m1$ space group) with increased lattice parameters $a = 13.328$ Å, $b = 7.580$ Å, $c = 12.860$ Å, and $\beta = 93.23°$, which corresponds to the superstructure $2\sqrt{3}a_0 x 2a_0 x 2c_0$ formed by ordering of Cr ions within vdW gaps.

In order to examine further the phase transition in $Cr_{0.25}TiTe_2$ we have made thermal expansion and specific heat measurements. The specific heat measurements have revealed the presence of a well defined, quite symmetrical peak on the C_p versus T dependence with a maximum at $T_t = 238$ K (shown in figure 10(a)). The thermal expansion data support the results of x-ray diffraction measurements. As can be seen in figure 10(b), the linear coefficient α of the thermal expansion for $Cr_{0.25}TiTe_2$ shows a pronounced anomaly at $T \sim T_t$. However, we did not observe any anomalies in the temperature dependences of the specific heat and thermal expansion for the parent compound $TiTe_2$ (also shown in figure 10).

It should be emphasized here that the phase transition in $Cr_{0.25}TiTe_2$ at T_t can hardly be associated with the order–disorder transition in the subsystem of intercalated Cr ions only. This is because the phase transition associated with disordering of guest atoms and vacancies in M_xTX_2

compounds is usually accompanied by the growth of the unit cell volume as well as by the increase of the electrical resistivity. Such a kind of order–disorder transition or 'melting' in the subsystem of intercalated M atoms was observed in several M_xTX_2 compounds, for instance, in $Cu_{0.5}NbS_2$ [28], $Ag_{0.66}TaS_2$ [29], and $Ni_{05}TiX_2$ (X = S, Se) [30]. In all these compounds the electrical resistivity shows an upturn at the order–disorder transitions when the temperature increases, which was ascribed to the growth of the scattering of charge carriers by statistically distributed M ions between TX_2 sandwiches. The opposite behavior of the resistivity in our $Cr_{0.25}TiTe_2$ sample implies that structural changes within Te–Ti–Te tri-layers may also be involved in the structural transition at T_t since some indications of the CDW instability were observed for $TiTe_2$ [4]. The CDW related energy gap may be responsible for the anomalous behavior of the resistivity observed in $Cr_{0.25}TiTe_2$.

4. Conclusion

The intercalation of Cr is observed to affect substantially the crystal structure and physical properties of the $TiTe_2$ compound. The insertion of Cr ions between Te–Ti–Te tri-layers leads to the reduction of the average interlayer distance, while the interatomic distance within layers is found to grow with increasing Cr concentration. These lattice deformations in Cr_xTiTe_2 differ substantially from that observed in the Cr_xTiS_2 system [20] in which the intercalation of Cr ions expands the lattice in the c direction. Such a difference may be attributed to the higher covalency degree of the bonds formed by Cr with adjusted chalcogen and Ti layers in Cr_xTiTe_2 in comparison with Cr_xTiS_2. At room temperature, the intercalated Cr_xTiSe_2 compounds exhibit the same crystal structure as $TiTe_2$ in the Cr concentration range $0 < x < 0.5$. The increase of the Cr content up to $x \geqslant 0.5$ leads to the appearance of a superlattice owing to the ordering of Cr ions and vacancies. At high Cr concentrations ($x \geqslant 0.33$), the Cr_xTiTe_2 compounds are observed to exhibit a ferromagnetic behavior with the Curie temperature up to 120 K for $x = 0.65$. The values of the effective magnetic moment of Cr intercalated into $TiTe_2$ are close to the expected spin-only value 3.87 μ_B for Cr^{3+}. This situation differs from that observed for M_xTiX_2 systems intercalated with other 3d metals in which lower μ_{eff} values are found in comparison with effective magnetic moments calculated in a local-moment model. The study of the electrical properties of Cr_xTiTe_2 has revealed the changes from metallic-like resistivity behavior to insulator-like with increasing Cr concentration above $x = 0.33$. Moreover, in the compound $Cr_{0.25}TiTe_2$, an anomaly in the temperature dependence of the electrical resistivity is observed at around 230 K. This anomaly is accompanied by a structural phase transition. An abrupt decrease of the resistivity with increasing temperature at this transition cannot be explained only by order–disorder effects within the subsystem of intercalated Cr ions since order–disorder transitions in other M_xTX_2 compounds are usually accompanied by a substantial growth of the resistivity. It should be mentioned that the resistivity anomalies, for example in $Cr_{0.25}TiTe_2$, were also observed in some other intercalated compounds, in particular, in M_xTiSe_2 (M = Mn, Cr) at $x \geqslant 0.33$ [31] and Fe_xVSe_2 at $x \geqslant 0.1$ [32]. In these systems, the intercalation of a small number of M atoms is observed to suppress the CDW state existing in the pure $TiSe_2$ and VSe_2 compounds. However, at higher intercalant concentrations ($x > 0.1$) anomalies of the resistivity were found again, which was ascribed to the reappearance of the CDW state [31]. Bearing in mind the above-mentioned results about the possible CDW instability of $TiTe_2$ [4] one can suggest that the anomalous resistivity behavior observed in the present work on $Cr_{0.25}TiTe_2$ samples originates in both the order–disorder transition in the Cr subsystem and structural changes associated with the CDW type transition in $TiTe_2$ sandwiches. In order to confirm our suggestion detailed crystal structure investigations on single crystalline samples are needed.

Acknowledgments

This work was partly supported by the Russian Foundation for Basic Research (grant No 09-02-00441-a) as well as by the program of the Ministry of Education and Science of the Russian Federation (Project No 2.1.1.1682).

References

[1] Friend R H and Yoffe A D 1987 *Adv. Phys.* **36** 1
[2] Wilson J A, Di Salvo F J and Mahajan S 1975 *Adv. Phys.* **24** 117
[3] Di Salvo F J, Moncton D E and Waszczak J V 1976 *Phys. Rev.* B **14** 4321
[4] de Boer D K G, van Bruggen C F, Bus G W, Coehoorn R, Haas C, Sawatzky G A, Myron H W, Norman D and Padmore H 1984 *Phys. Rev.* B **29** 6797
[5] Koike Y, Okamura M, Nakanomyo T and Fukase T 1983 *J. Phys. Soc. Japan* **52** 597
[6] Perfetti L, Rojas C, Reginelli A, Gavioli L, Berger H, Margaritondo G, Grioni M, Gaa'l R, Forro L and Rullier-Albenque F 2001 *Phys. Rev.* B **64** 115102
[7] Strocov V N, Krasovskii E E, Schattke W, Barrett N, Berger H, Schrupp D and Claessen R 2006 *Phys. Rev.* B **74** 195125
[8] Arnaud Y and Chevreton M J 1981 *Solid State Chem.* **39** 230
[9] Kim Y S, Mizuno M, Tanaka I and Adachi H 1998 *Japan. J. Appl. Phys.* **37** 4878
[10] Shannon R D 1976 *Acta Crystallogr.* A **32** 751
[11] Morosan E, Zandbergen H W, Dennis B S, Bos J W G, Onose Y, Klimczuk T, Ramirez A P, Ong N P and Cava R J 2006 *Nat. Phys.* **2** 544
[12] Inoue M, Hughes H P and Yoffe A D 1989 *Adv. Phys.* **38** 565
[13] Negishi H, Shoube A, Takahashi H, Ueda Y, Sasaki M and Inoue M 1987 *J. Magn. Magn. Mater.* **87** 179
[14] Pleschov V G, Baranov N V, Titov A N, Inoue K, Bartashevich M I and Goto T 2001 *J. Alloys Compounds* **320** 13
[15] Maksimov V I, Baranov N V, Pleschov V G and Inoue K 2004 *J. Alloys Compounds* **384** 33
[16] Rodriquez-Carvayal J 1993 *Physica* B **192** 55
[17] Danot M, Rouxel J and Gorochev O 1974 *Mater. Res. Bull.* **9** 1383
[18] Calvarin G, Gavarri J R, Buhannic M A, Colombet P and Danot M 1987 *Revue Phys. Appl.* **22** 1131
[19] Pleschev V G, Selezneva N V, Maksimov V I, Korolev A V, Podlesnyak A V and Baranov N V 2009 *Phys. Solid State* **51** 933

[20] Inoue M and Negichi H 1986 *J. Phys. Chem.* **90** 235
[21] Sherokalova E M, Pleschov V G, Baranov N V and Korolev A V 2007 *Phys. Lett.* A **369** 236
[22] Pleshchev V G, Korolev A V and Dorofeev Yu A 2004 *Phys. Solid State* **46** 280
[23] Kuznetsova T V, Titov A N, Yarmoshenko Yu M, Kurmaev E Z, Postnikov A V, Pleschev V G, Eltner B, Nicolay G, Ehm D, Schmidt S, Reinert F and Hüfner S 2005 *Phys. Rev.* B **72** 085418
[24] Rossiter P L 1981 *J. Phys. F: Met. Phys.* **11** 2105
[25] Yadav C S and Rastogi A K 2008 *J. Phys.: Condens. Matter* **20** 465219
[26] Di Salvo F J and Waszczak J V 1976 *J. Physique* C4 **37** (Suppl.) 157
[27] Di Salvo F J, Wilson J A and Waszczak J V 1976 *Phys. Rev. Lett.* **36** 885
[28] Pfalzgraf B W, Spreckels H, Paulus W and Schollhor R 1987 *J. Phys. F: Met. Phys.* **17** 857
[29] Boebinger G S, Wakefield N I F, Marseglia E A and Friend R H 1983 *Physica* B+C **117/118** 608
[30] Plovnick R H, Perloff D S, Vlasse M and Wold A 1968 *J. Phys. Chem. Solids* **29** 1935
[31] Baranov N V, Maksimov V I, Mesot J, Pleschov V G, Podlesnyak A, Pomjakushin V and Selezneva N V 2007 *J. Phys.: Condens. Matter* **19** 016005
[32] Yadav C S and Rastogi A K 2008 *J. Phys.: Condens. Matter* **20** 415212